A Contribution to the Understanding of the Grinding of PcBN – Influence of Diamond Specification on Wear during Peripheral Grinding

Berend Denkena, Alexander Krödel-Worbes, Dominik Müller-Cramm*
Institute of Production Engineering and Machine Tools, Leibniz Universität Hannover, An der Universität 2, 30823 Garbsen, Germany.

* Corresponding author. Tel.: +49 511 762 2553; email: mueller-cramm@ifw.uni-hannover.de
Manuscript submitted June 29, 2022; accepted November 29, 2021.
doi: 10.17706/ijmse.2022.10.3.42-56.

Abstract: When grinding brittle-hard polycristalline boron nitride (PcBN), high wear occurs on the grinding tool. The high wear is caused by the small difference in hardness between the PcBN and the diamond abrasive, as well as the higher hot hardness of the PcBN. This paper investigates the grinding behavior during peripheral traverse face grinding of PcBN with vitrified bonded diamond grinding tools. Therefore, the diamond grain shape, size and concentration are varied. The investigations are conducted with a PcBN specification with 70% cBN content. The grinding process is evaluated by analyzing both the process force components and the wear characteristics of grain, profile and edge wear. The results of this study reveal a significant influence of the diamond grain shape and size. For selected test points, a low profile wear $G > 14$ and edge wear $r_{sk} < 2 \cdot d_g$ is observed.

Key words: Peripheral grinding, PcBN, wear, vitrified grinding tool.

1. Introduction

Polycrystalline cubic boron nitride is a composite of the hard material cubic boron nitride (cBN), which is bound by a binder matrix material. The hard material cBN has a similar crystal structure and properties to diamond. In contrast to diamond, cBN is thermally stable up to a temperature of 1,500 to 1,600 °C [1]. The hardness of cBN is up to 80% of diamond. At room temperature it has a Knoop hardness of up to $HK = 45$ GPa in the single crystal [2].

Ceramic binders consist mainly of titanium nitride, TiN, aluminum nitride AlN or mixed ceramics such as Ti(C,N). These PcBN specifications have a low thermal conductivity and a high heat resistance up to 1500 °C [3], [4]. Metallic binders are based on cobalt Co, tungsten W or nickel Ni. The carbides TiC and WC are also used as matrix materials to achieve higher resistance against abrasive wear. This kind of binder matrix is more ductile than ceramic binder materials [5].

Early work in this area focused primarily on the material properties of PcBN grains. It was shown that its hardness primary depends on the cBN content C_{cBN}. The range of the vickers hardness of PcBN is 2500 HV02 for $C_{cBN} = 50\%$ to 5500 HV02 for $C_{cBN} = 90\%$ [6]. The fracture toughness of the material is typically in the range of $K_{IC} = 3{,}7$ to $13{,}5$ MPa · m$^{0.5}$. It has been demonstrated that the fracture toughness generally decreases with both increasing cBN particle size d_{cBN} and increasing binder content [7]. There is a difference between

the two materials diamond and cBN in their different chemical affinity to ferrous metals. When diamond is used as a cutting material for ferrous metals, tribochemical wear occurs as a result of the high diffusion tendency of carbon into ferrous metals. In contrast, cBN shows no reactivity with ferrous metals. This allows cBN to be used for hard machining of steel components and nickel-based alloys [6].

Furthermore, PcBN is highly resistant towards abrasive wear due to its high hardness [5]. As a result of its mechanical, thermal and chemical properties, PcBN is suitable as a cutting material for the machining with geometrically defined cutting edge. PcBN specifications adapted to these processes differ in the particle size and content of the cBN as well as the composition of the binder [8]. PcBN specifications with ceramic binders have low thermal conductivity and high resistance to abrasive wear.

Regarding modern cutting tools, PcBN is mainly used for indexable cutting inserts. The geometry of the inserts is usually generated by plunge face grinding [9]. Because of of the high hardness of the PcBN, each individual grain engagement leads to significant wear on the diamond grain. In the case of vitrified bonded diamond grains, the profile wear of the abrasive layer correlates with the quotient of the equivalent chip thickness h_{eq} and the contact length l_g, which in turn is inverse proportional to the velocity ratio q according to (1).

$$G \sim h'_{eq} = h_{eq}/l_g \sim 1/q \ = v_{fa}/v_c \tag{1}$$

From (1), the contact length specific equivalent chip thickness h'_{eq} can be increased by reducing the cutting speed v_c and by increasing the feed rate v_{fa}. Increasing h'_{eq} leads to a higher mechanical load on the abrasive grain. Due to the higher mechanical load, the diamond grain splinters and generates new cutting edges. Consequently, by increasing h'_{eq} a G-ratio of $G > 4$ has been achieved. This is eight times higher than the previous state of the art [10]-[12]. The specific grinding energy e_c increases and the grinding force ratio μ decreases by increasing the axial feed rate v_{fa} [13]. In a geometrical consideration, h'_{eq} can be increased by a reduction of the geometrical contact length l_g by varying the cutting direction angle leads to a shorter contact time. The diamond grain is subjected to less thermal stress by shortening the contact time. As a result, the reduction of l_g leads to less grain flattening and reduces the amount of grain breakouts and thus the profile wear of the grinding tool [14].

The grinding of polycrystalline diamond (PCD) shows similar wear mechanisms on the grinding tool as the grinding of PcBN. Investigations of the PCD specification CTB010 with vitrified bonded diamond grinding tools of grain size D15 (d_g = 12 µm to 15 µm) show a high initial wear. This initial wear rate decreases degressively and changes to a linear wear rate as the machining time progresses. The linear wear rate during machining is caused by a flattening of the abrasive grains. The G ratio decreases as the cutting speed and feed rate increase [15]. Investigations on the grinding of PCD *by Vits* show that increased grain splintering and bond breakage occurs as initial wear. This initial wear is followed by flattening of the abrasive grains due to abrasion [16]. Furthermore, the vitrified bonded abrasive layer is elastically compressed under the load of the grinding normal forces. Abrasion of the abrasive grains and diamond particles in the workpiece occurs when they slide over each other. However, when an abrasive grain hits a void in the material, the abrasive layer expands locally, forcing the abrasive grain into the void. This leads to a sudden increase in load when the abrasive grain hits a PCD-grain behind the void. This overloads the abrasive grain, causing it to splinter or break out [17].

While the process variables have a significant influence on the tool wear, no significant influence of the abrasive layer specification could be determined. For this purpose, the bond hardness, the diamond grain size and the grain concentration were varied [12]. The previous investigations refer to plunge face grinding, which is used to machine PcBN inserts [11], [12], [14]. Circumferential grinding processes are used for machining PcBN shank tools and these grinding processes have not been investigated so far. Shank tools with small

diameters are used for hard fine machining of steel. The heads of such shank tools are made of PcBN solid material [18]. A milling cutter generally has flutes that are produced by spark erosion or longitudinal peripheral grinding. In contrast to plunge face grinding, in peripheral grinding the chip thickness varies locally [9]. Thus, the geometry of the contact zone between the grinding tool and the workpiece differs from the contact zone in plunge face grinding.

As a result of the different engagement conditions compared to plunge surface grinding, the chip thickness varies over the longitudinal chip section. In addition, the contact length l_g can be reduced to a much greater extent by reducing the infeed than in plunge face grinding. Therefore, it can be assumed that the load for the diamond abrasive during peripheral grinding of PcBN is different from the load during plunge face grinding. Flute grinding, i.e. peripheral grinding, is a finishing operation for PcBN workpieces. Therefore, for a true contour manufacturing of the flute, it is necessary to find suitable abrasive layer specifications and to investigate their influence on the grinding process. Therefore, in this study, the influence of the abrasive layer specification on the wear on the grinding tool during longitudinal peripheral grinding of PcBN is determined.

2. Experimental Setup and Methods

As an analogy to the grinding of complex flute geometries, longitudinal surface grinding in part engagement is used as a test setup (Fig. 1). One edge of the grinding layer is engaged together with a part of the lateral surface. The other part of the grinding tool does not participate in the machining of the PcBN workpiece.

The experiments are carried out on a three-axis CNC surface grinding machine FS 840 KT CNC from Geibel & Hotz GmbH. The machine features high precision and repeatability due to its rigid design and integrated grinding and dressing cycles. This is required since comparatively high process forces are to be expected for the grinding of PcBN. With a spindle power P_s = 14 KW, any speed fluctuations due to these high forces should be minimized. Additionally, the minimum grinding spindle speed is n_s = 1000 min^{-1}, so that very low cutting speeds can be realized. The workpieces are clamped via a clamping device made of prehardened cold work steel (Fig. 1a). The fixture enables repeatable clamping over the length of the workpiece.

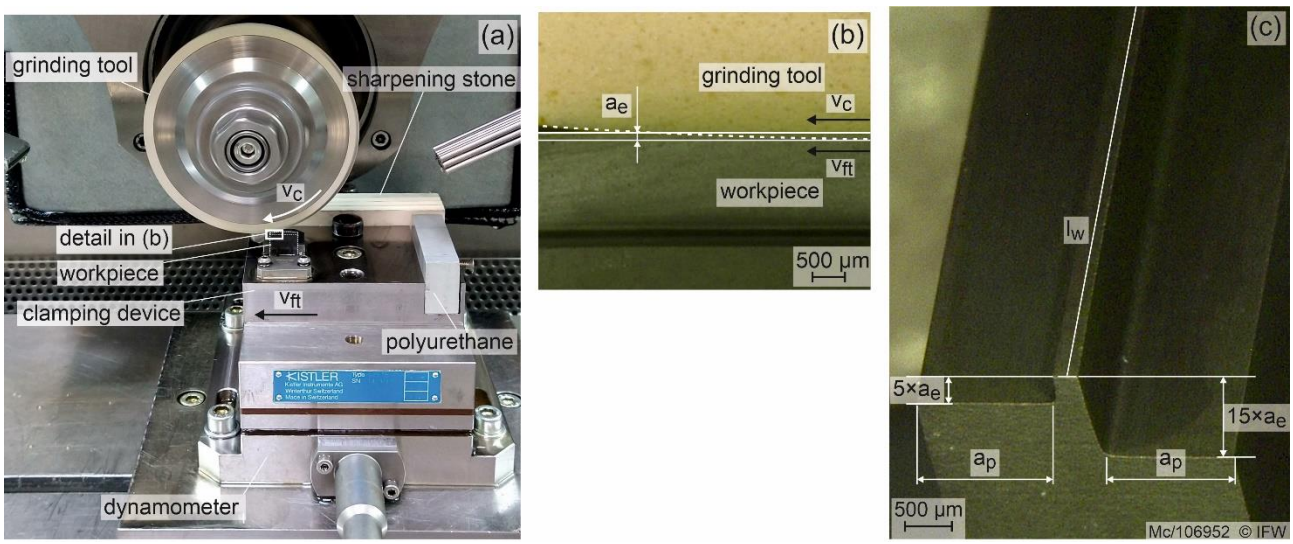

Fig. 1. Experimental setup a) overview, b) contact zone, and c) ground workpiece.

The ground workpieces are S-shaped PcBN inserts with a cBN content C_{cBN} = 70% of solid material. The workpieces have a length of l_w = 13 mm and a width of b_w = 3.2 mm (Fig. 1b and Fig. 1c). The hardness is determined by means of a Qness Q10A+ hardness tester. The respective specification and hardness are summarized in Table 1.

Table 1. Experimental Setup

Parameter	Value
properties of PcBN	
cBN content C_{cBN}	70%
cBN particle size d_{cBN}	2 µm
hardness *HV0.2*	3736 ± 204
process variables	
cutting speed v_c (m/s)	10
feed rate v_{ft} (mm/min)	180
depth of cut a_e (mm)	0.1
length of the workpiece l_w (mm)	13
spec. material removal V'_w [mm^3/mm]	2.5 to 19.5
spec. material removal rate Q'_w [mm^3/mm · s]	0.25

For the machining of the PcBN, vitrified bonded diamond grinding tools with different abrasive layer specifications regarding grain concentration C, grain size d_g and grain shape are used. The used diamond grain types M and L and the grain diameter distributions are shown in Fig. 2. The diamond grain L (Fig. 2a and Fig. 2c) in general is irregularly shaped. For the grain size d_g = 15 µm, the diamond grain is plate-shaped. It has conchoidal fracture faces on the plate sides and irregular fracture edges on the side faces. At a grain size of d_g = 25 µm the diamond grain is needle-shaped. It has very irregularly shaped fracture surfaces on the entire surface.

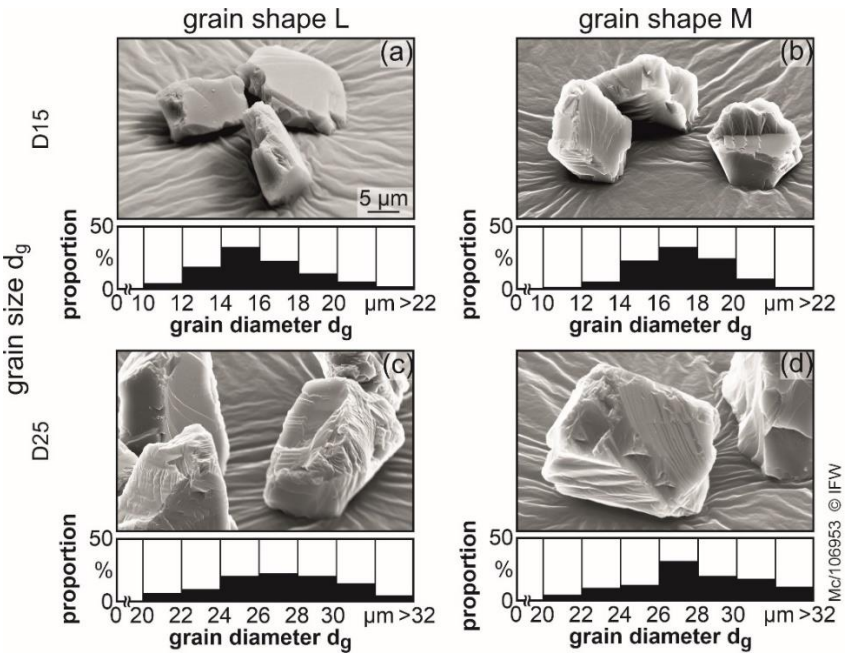

Fig. 2. SEM pictures of the grain shapes L and M.

The grain shape of the diamond grain M also is irregular, but with a narrower grain size distribution (Fig. 2b and Fig. 2d). Its fracture strength, which is indicated by the grain manufacturer, is higher than for the grain shape L. In both grain size d_g = 15 µm and 25 µm, the shape of the diamond M grain is rather isometric and can be described as an irregular octahedron. It shows irregular fractures at the edges. The diamond grain has irregularly shaped fracture surfaces, which indicate a lower fracture tendency than for the L grain.

The profiling of the grinding tools is performed using a multilayer diamond form roll with CVD diamond reinforcement on one edge. A dressing speed ratio q_d = −6 and an overlap ratio U_d = 6 are defined. Sharpening

is achieved with a sharpening stone made of white high-grade corundum with 1000 mesh (Fig. 1a). The sharpening volume related to the contact width a_p is V'_S = 30 mm^3/mm in each case.

Mineral oil with a low viscosity of υ = 9.2 mm^2/s is used as the cooling lubricant. The cooling lubricant is fed into the contact zone by needle nozzles with a volume flow of Q = 5 l/min.

During grinding, the grinding tool engages the respective workpiece at a width of cut a_p = 1.55 mm, resulting in strain on both, the cylinder profile and the edge of the abrasive layer. Thus, the resulting edge wear can be determined for the respective test. The method for determining edge wear is described later in the article. The set process variables are listed in Table 1. A total specific material removal V'_w = 19.5 mm^3/mm is removed in 15 tool engagements in each grinding test. The microscopic and macroscopic tool wear is determined after five, ten, and fifteen tool engagements corresponding to the specific material removal V'_w = 6.5, 13.0, and 19.5 mm^3/mm. Each test is performed in triplicate.

For determining microscopic tool wear, the topography of the outer surface of the grinding layer is measured. An Alicona InfiniteFocus G5 white light microscope with focus variation is used for this purpose. Subsequently, an area-based Abbott-Firestone curve is determined from the topography of the abrasive layer. The wear of the grain peaks is investigated by the reduced peak height *Spk* and the volume of the peaks *Vmp*. A reduction of *Vmp* can be considered as an indication of grain splintering. A reduction of *Spk* and *Vmp*, on the other hand, is an indication of grain flattening. Clogging of the chip spaces can be determined from the reduced valley depth *Svk* and the volume of the grooves *Vvv*. A reduction in *Svk* and *Vvv* is an indication of reduced chip space, which can only occur through clogging when grinding with highly porous vitrified grinding tools.

For determining macroscopic tool wear, the grinding wheel contour is ground into a polyurethane workpiece with a fine cell structure each time after sharpening and after grinding the PcBN workpieces (Fig. 1 a). Subsequently, the profile and edge wear are measured on the profiles ground into the polyurethane workpieces. Before each test, the grinding tool profile is ground and the edge radius is determined. After grinding the PcBN, the worn profile is ground and the new edge radius is determined. Subsequently, the edge radii are subtracted from each other.

During the grinding process, the tangential and normal cutting force components are also recorded using the Kistler 9257B three-component dynamometer (Fig. 1a). The clamping system is mounted flat on the force measuring system. Its flat, large-area mechanical connection enables low-damping force transmission between the workpiece and the force measurement system. The respective arithmetic mean value of the grinding force is calculated. Grinding forces are considered in the steady-state range solely to exclude the influence of the initial grinding process on the mean value of the forces. For the evaluation of the grinding process, the specific grinding normal forces $F'_n = F_n/a_p$, the specific cutting energy $e_c = P'_c/Q'_w$ and the grinding force ratio $\mu = F_t / F_n$ are evaluated. The specific grinding normal force F'_n is considered as an indicator for the mechanical stress of the bond, since with an increase of F'_n higher stresses act in the bond bridges between the abrasive grains. The grinding force ratio μ together with the specific cutting energy e_c allows conclusions to be drawn about the thermal load on the abrasive grains due to friction. As shown by *Denkena et al.* [14], without changing the test setup microwear leads to an increase of e_c with the increasing V'_w due to an increasing share of friction in the total cutting energy.

Each grinding test consists of five steps: profiling, sharpening, determining the original tool profile, PcBN grinding, determining the worn tool profile.

3. Results and Discussion

3.1. Topography of the Abrasive Layer

The engagement of the diamond grains in the PcBN not only leads to material removal from the workpiece,

but also to changes in the abrasive layer surface. As an example, Fig. 3 compares the initial state, (a) and (c), and the worn state, (b) and (d), of both grain shapes L and M for grain size d_g = 15 µm. Both dressed topographies (a) and (c) have a high grain protrusion. The pore structure of the abrasive layer is clearly distinguishable from the closed surface as clearly defined cavities. Both worn states (b) and (d) show a high proportion of opened pores that increase the topography parameter *Svk*, the reduced valley depth. Pores accessible from the surface increase the available chip space of the abrasive layer topography. Hence, more chip space is available for removing ground material from the contact zone. However, the worn topographies of both grain shapes differ in the microwear of the abrasive grains. While grain shape M continues to have an irregular topography with high grain protrusion, the surface of grain shape L consists mainly of flattened grains forming leveled plateaus. This is also reflected in the surface parameter *Spk*, the reduced peak height. This parameter is reduced in grain shape M compared to the initial state, but still at a high level. For grain shape L, on the other hand, the parameter *Spk* is reduced to far below 1 µm. The plate-shaped grain of specification L leads to a strong flattening of the grains during grinding. Since the grain is broken in itself without being released from the bond, the flattened plateaus are formed. The more compact, octahedron-shaped grain of specification M splinters during the process. Thus, new sharp cutting edges are generated. Due to its more compact shape than the grain of grain shape L, the grain is released sooner when it is flattened.

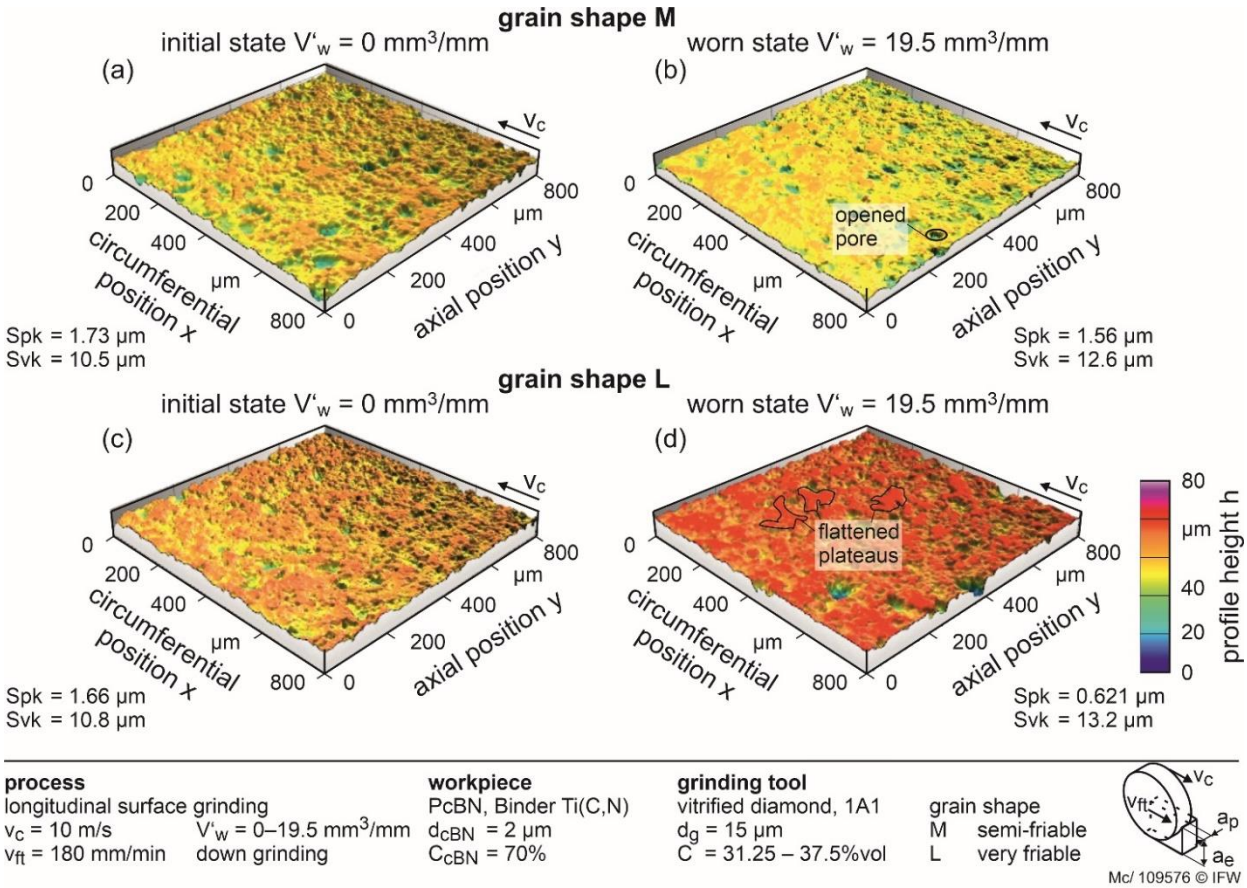

Fig. 3. Influence of the grain shape on the grinding layer topography for grain size d_g = 15 µm.

The same trends of microscopic wear can be seen when comparing the topographies of both grain specifications M and L in the grain size d_g = 25 µm. As an example, the topographies of the grinding tools are shown initially and after completion of the test in Fig. 4. Here, even a higher initial grain protrusion can be observed for the very friable grain of the specification L than for the semi-friable grain of the specification M. The irregular and needle-shaped grain of specification L has a wide grain size distribution. It produces sharp

cutting edges protruding further from the abrasive layer surface with the same grain centering as the M grain shape. On the other hand, the more compact, regular shape of specification M after dressing results in a more uniform distribution of grains in the abrasive layer surface and thus in less grain protrusion than with specification L. With the worn abrasive layer of specification L (d), the same effect is seen with regard to the opened pore spaces as for the diamond grain size d_g = 15 µm. Initially closed pore spaces are opened by bond fractures. These increase the chip space in the abrasive layer topography. In the case of grain specification M, the pores in the grinding layer topography are already open initially after dressing (a). This is reflected in the high value of *Svk* = 13.8 µm. During grinding, the chip spaces formed by the pores become clogged with ground particles, so that the depth of the chip spaces is reduced. This is reflected in a lowering of the surface parameter to *Svk* = 11.4 µm.

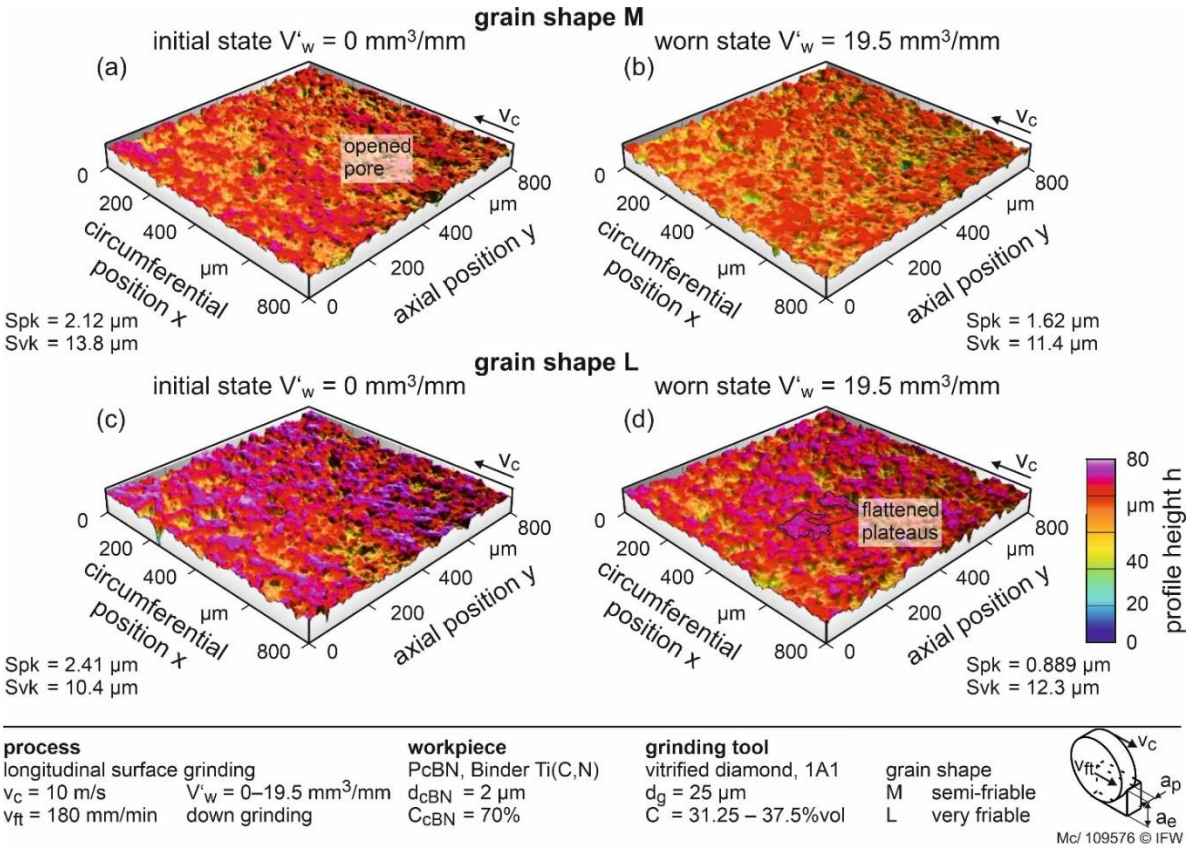

Fig. 4. Influence of the grain shape on the grinding layer topography for grain size d_g = 25 µm.

To evaluate this change with increasing material removal V'_w, the reduced peak height *Spk*, reduced valley depth *Svp*, peak volume *Vmp*, and void volume of the grooves *Vvv* are compared from V'_w = 0 mm^3/mm to V'_w = 19.5 mm^3/mm. Fig. 5 depicts the progression of the four surface parameters with increasing material removal for both grain shapes M and L and both grain sizes d_g = 15 µm and 25 µm.

The diamond grain L shows a very different progression at grain size d_g = 15 µm compared to grain size d_g = 25 µm. The topography at d_g = 25 µm changes slightly with increasing material removal. In contrast, a significant decrease in both *Spk* and *Vmp* is observed at d_g = 15 µm. The decrease in both surface parameters can be attributed to the flattening and splintering of the very friable grain under the load in engagement. It is less mechanically stable, so that individual dominant diamond grains protruding from the surface are sheared off in contact with the very hard PcBN. The diamond grain is flattened and consequently less sharp. With grain shape L, the surface parameters *Svk* and *Vvv* do not change substantially. This indicates that only minor clogging of the chip space occurs during grinding.

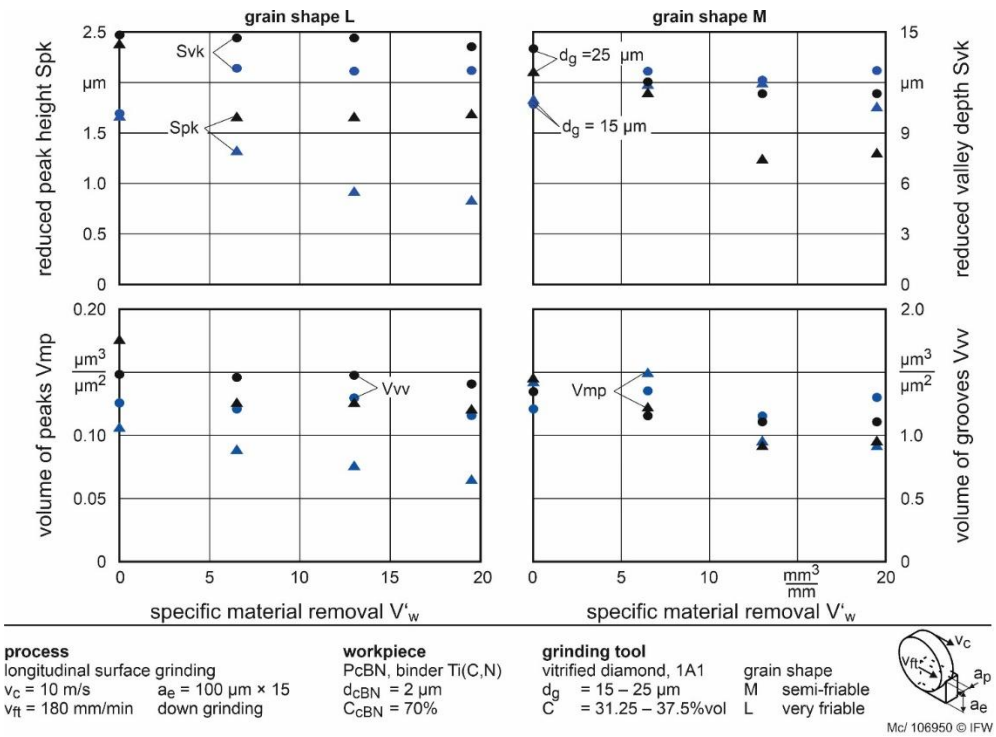

Fig. 5. Influence of the specific material removal on the topography parameters of the abrasive layer.

With grain shape M, the different diamond grain sizes show a different behavior from grain shape L. With both, small and large grain sizes, significantly higher values of *Spk* and *Vmp* are present after V'_w = 6.5 mm^3/ mm. This indicates that even after one third of the grinding process, significantly more sharp cutting edges protrude from the abrasive layer than with grit shape L. At V'_w = 13 mm^3/mm, a static state is reached where no further flattening of the diamond grains occurs. For grain size d_g = 15 µm, this flattening occurs at a 0.5 µm higher level than for d_g = 25 µm. This means that the envelope of the abrasive layer is located radially more to the outside. For the grain diameter d_g = 15 µm, the average grain density in the contact zone is about 150% higher than for grain diameter d_g = 25 µm. Thus, with a small grain size d_g = 15 µm, considerably more grains are involved in the grinding process. Therefore, the single grain chip thickness is lower. Consequently, the wear on the diamond grain occurs at a higher distance from the bond level.

Taking into account the conclusions for grain shape M, it is assumed that for grain shape L of grain size d_g = 25 µm the steady state of wear is already reached at V'_w = 6.5 mm^3/mm. There is no change in the topography parameters, because in the interval V'_w = 0 to 6.5 mm^3/mm the significant changes in the abrasive layer surface have occurred. The needle-shaped grain of specification L is thus broken early and forms flattened plateaus. Thus, the micro-wear mechanism on the diamond grain in peripheral grinding is different from that in plunge face grinding. While a dulling of the cutting edges of the diamond grain can be observed in plunge face grinding [11], [14], grain flattening under mechanical overload or grain breakout and the associated self-sharpening of the abrasive layer surface is more likely to occur in circumferential grinding under the selected process variables.

The change in the abrasive layer topography directly influences the process parameters. The following section therefore shows the progression of the process force components and the cutting energy derived from the process parameters.

3.2. Process Parameters

Microwear on the diamond grain results in a change in the contact conditions between the abrasive layer and the workpiece. With increasing grain flattening, the contact area of the grains and the bond increases.

This has an effect on the specific cutting energy and the grinding forces. The relationship between the specification of the abrasive layer and the thermomechanical load in grinding PcBN is investigated using an analysis of the process forces and process parameters derived from the forces. When considering the specific grinding energy of the two abrasive layers presented in Fig. 6, the transition of the initial wear phase to the constant wear rate can be derived.

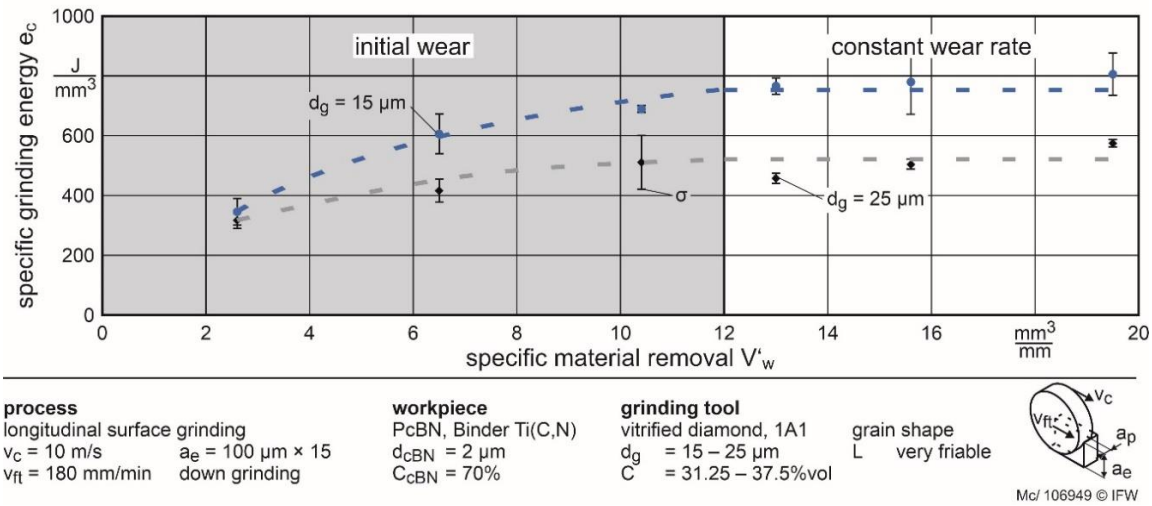

Fig. 6. Specific grinding energy of the abrasive layers with increasing specific material removal.

Since the standard deviations of the two grinding energies overlap at the beginning of the grinding process at V'_w = 2.6 mm^3/mm, a similar initial grinding energy level can be assumed. A similar dressing results can be expected in terms of available chip space and grain embedding, since both abrasive layers are dressed in the same way. With increasing material removal V'_w microwear occurs on the surface of the abrasive layer. Grain flattening and grain breakout are identified as the predominant microwear mechanisms in Section 3.1. Grain breakout leads to profile wear, but it exposes new sharp abrasive grains. Flattening of the diamond grains increases friction in the contact zone between the abrasive layer and the workpiece. Since grain flattening can also lead to grain breakout from the brittle vitrified bond, an equilibrium is reached during grinding as the material removal V'_w increases. The resulting constant wear rate is observed for all investigated grinding layer specifications. Fig. 7 depicts the initial grinding energy $e_{c,0}$ and the grinding energy $e_{c,e}$ at equilibrium.

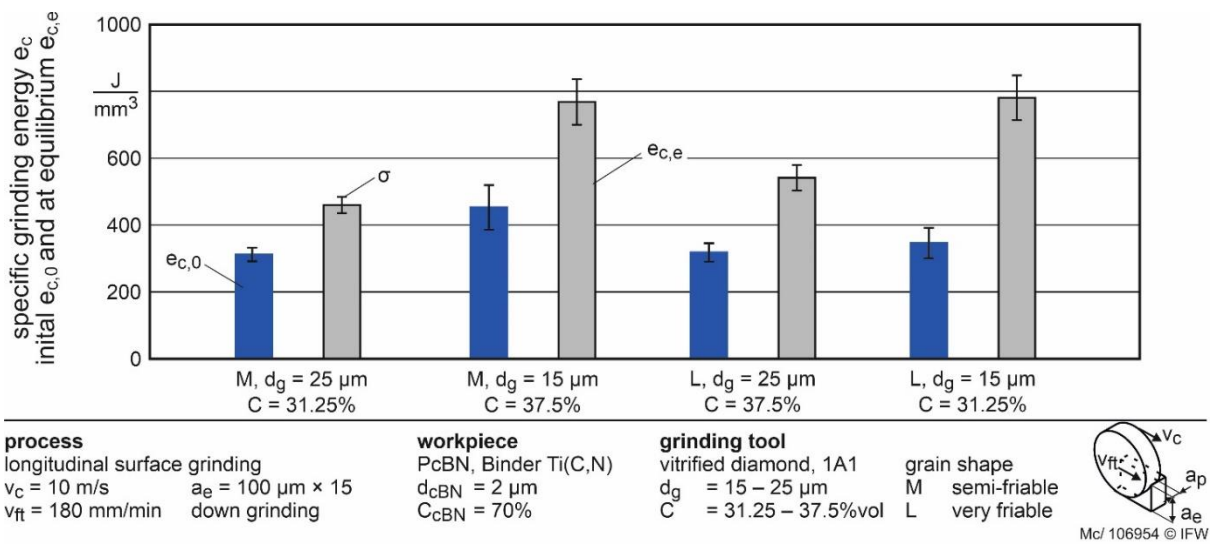

Fig. 7. Influence of the grain shape, grain size and wear state on the specific grinding energy.

The initial grinding energy $e_{c,0}$ of all abrasive layer specifications is significantly lower than the grinding energy at the equilibrium $e_{c,e}$. Furthermore, $e_{c,e}$ is 50% higher at the small diamond grain size of d_g = 15 µm than at the diamond grain size of d_g = 25 µm. The higher increase of the specific grinding energy at the smaller diamond grain size indicates an increased share of friction in the cutting process. Grain flattening increases the friction part of the cutting process. Considering the changes in the grinding surface topography, the wear mechanism of grain flattening can be identified as a major cause for the increase in grinding energy between initial state and constant wear rate.

As a result of the specific wear mechanism in the peripheral grinding of PcBN, there are changes in the grinding force. Thus, the impact of the wear progression on the grinding force ratio µ is presented next. Fig. 8 shows a decreasing grinding force ratio for grain shape M with increasing V'_w until a constant wear rate is reached at V'_w > 13 mm^3/mm. It should be noted that the components of the grinding force for different grain sizes and concentrations start at the same force level, as shown for the specific grinding energy e_c.

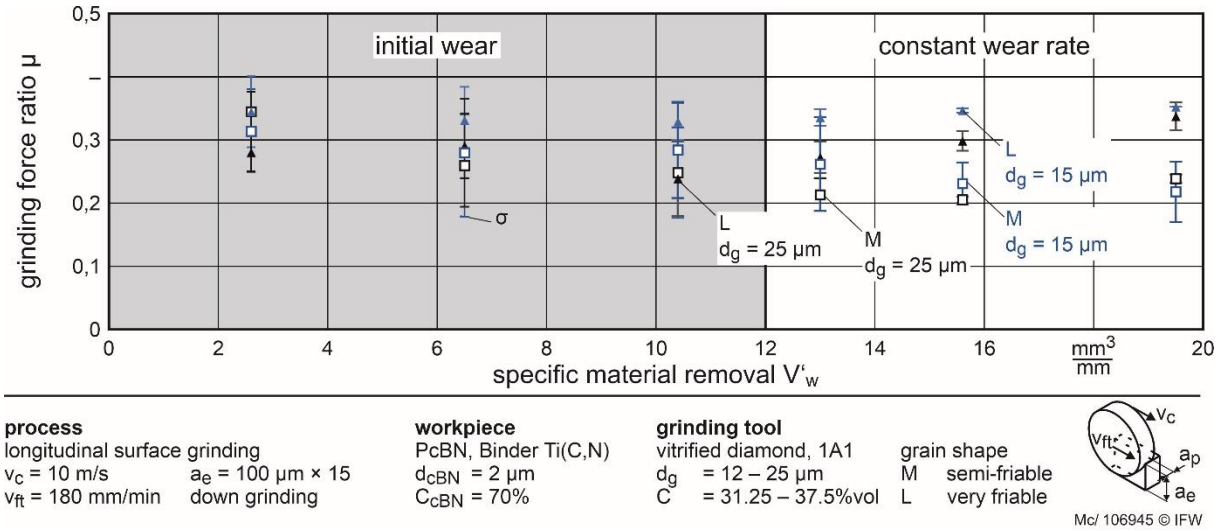

Fig. 8. After initial wear the specific grinding forces reach a constant level.

For grain shape L in grain size d_g = 25 µm the grinding force ratio increases with V'_w. As described in the consideration of the surface parameters these grains are flattened after initial grinding contact. Also, the specific cutting energy e_c of this grain specification is only increasing slightly with increasing material removal V'_w. The grain protrusion is low due to the strong grain flattening, which means that bond also comes into grinding contact. Therefore, the tangential grinding force component increases with V'_w due to the increasing friction between the grinding layer and the workpiece. The grain diameter d_g = 15 µm of grain shape L, on the other hand, has a constant high grinding force ratio. The cutting energy increases significantly during initial wear and the peak height of the abrasive layer topography decreases continuously. This correlation of observations indicates the splintering and flattening of the grain. The splintering counteracts the flattening of the grain, so that the total number of active cutting edges increases. With the increase in the number of active cutting edges, both process force components tangential and normal increase proportionally.

In contrast to the progressive wear of plunge face grinding [14], a constant wear rate can be observed in the circumferential grinding of PcBN after the initial wear. The wear progress is thus similar to the observations made when machining PCD [15]-[17]. As described in Section 3.1, grain splintering initially occurs when machining both PcBN and PCD materials. During the subsequent steady state, a flattening of the diamond grains is observed. When grinding PcBN, however, grain breakout also occurs, so that sharp diamond grains are provided again.

The cutting forces and the cutting force ratio are calculated in the described state of equilibrium for all investigated abrasive layer specifications. The cutting force ratio is used to compare the effectiveness of the cutting process. A high cutting force ratio at a low level of specific cutting energy indicates low friction and high separation energy shares of the total cutting energy. The results are depicted in Fig. 9. Under the same test conditions, the respective components of the grinding force differ significantly. The abrasive layer specification d_g = 25 µm, C = 31.25%vol, grain shape M has a higher grinding force ratio μ = 0.44 than the other abrasive layer specifications. Machining with sharp abrasive grains leads to a high tangential force and a low normal force. Grain flattening leads to a larger contact area and thus an increasing normal force component. This reduces the grinding force ratio. If a different number of abrasive grains are engaged under otherwise identical test conditions, both the tangential and the normal force components increase. Thus, no effect on the grinding force ratio can be observed. Therefore, it can be assumed that the wear mechanism of microwear is the same, but the wear rate differs.

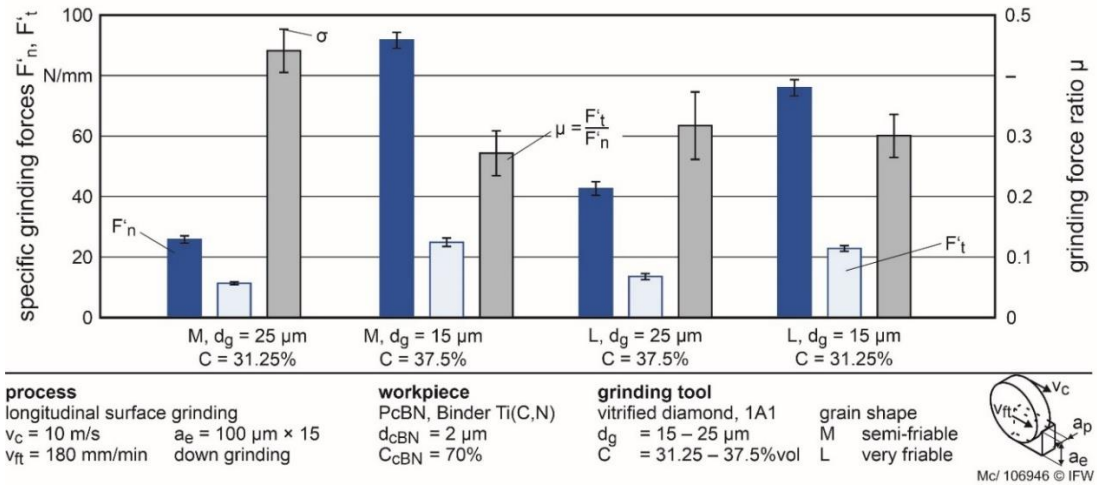

Fig. 9. Grinding forces and force ratio.

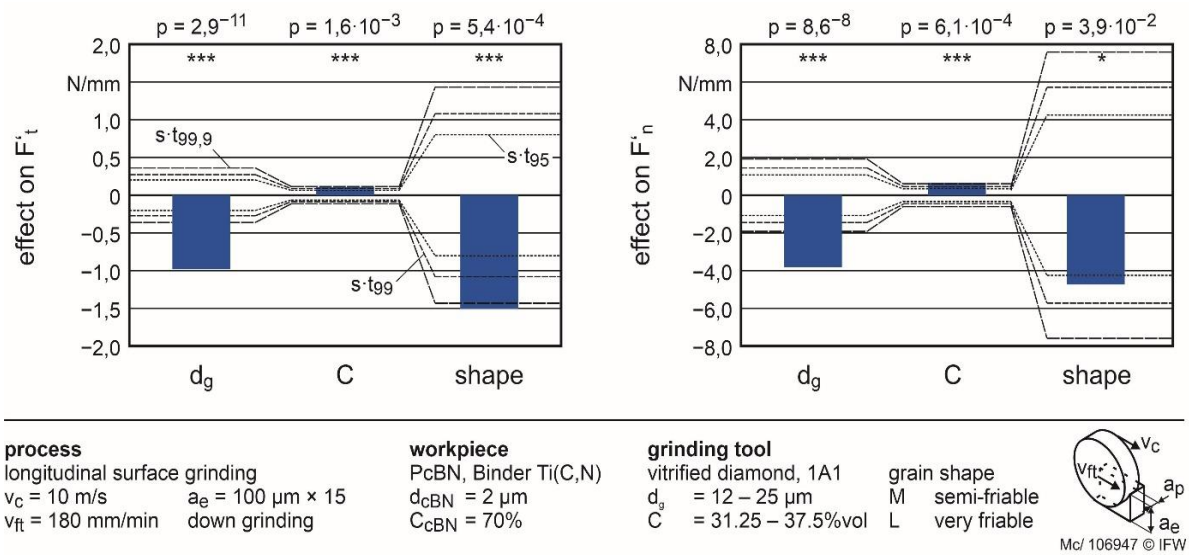

Fig. 10. Effect of the grinding layer specifications on the grinding forces. (*) low significance to (***) high significance.

For further analysis, the effects of abrasive grain size d_g, concentration C and shape are shown in Fig. 10. All three input variables have a highly significant effect on the tangential component of the grinding force. Here, the influence of grain size and shape are significantly higher compared to the influence of the grain

concentration. The measurement results are filtered using outlier tests. This leads to different confidence intervals for the investigated influencing variables.

The tangential force decreases with the size of the grains, as shown in Fig. 9. Also, the very friable grain L leads to significantly reduced tangential forces compared to the semi-friable grain shape M. For the normal components of the grinding force, basically the same effects can be demonstrated. However, the influence of the grain shape on the specific normal force is only slightly significant (p = 0.039). As described before, a larger grain diameter leads to a lower number of active diamond grains in the grinding process. Therefore, both the tangential and the normal force decrease with increasing grain diameter. Furthermore, increasing the grain concentration also leads to an increase in the number of active diamond grains in the grinding process. Thus, the process force components increase with the grain concentration. The influence of grain shape on F'_t is highly significant. The tangential grinding force component is composed of the cutting and friction components. The very brittle diamond grain L tends to splinter strongly during grinding, resulting in a leveled abrasive layer surface. The leveled abrasive layer surface increases the friction component of the tangential force, so that the tangential forces are higher on average than for diamond grain M. In summary, the microwear on the abrasive grain M is thus lower than on the abrasive grain L. The abrasive grain M enables more effective grinding of PcBN than the abrasive grain L over the investigated material removal V'_w.

3.3. Macroscopic Wear

The observed wear mechanisms during peripheral grinding of PcBN do not only influence the process forces and cutting energy. The flattening of the diamond grains also leads to breakout of the grains and thus to profile and edge wear on the abrasive layer. Figure 11 shows the grinding ratio G and the edge wear of the grinding tool. For the same cutting volume, a higher G-ratio means lower profile wear on the grinding tool. A high scattering of the G-ratios is shown, whereby for the abrasive grain shape M, d_g = 25 µm and C = 31.25%vol a grinding ratio of maximum G = 14.3 is obtained. Generally, when using abrasive grain M, on average 110% higher G-ratios are achieved than when using abrasive grain L since the very friable grain L has a higher wear rate than grain shape M.

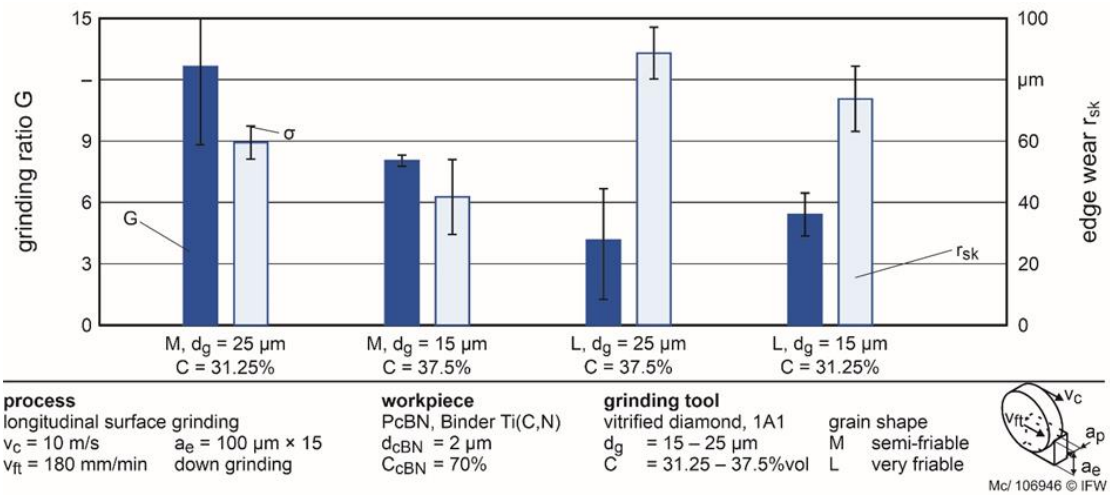

Fig. 11. G ratio and edge wear of the diamond grinding tools.

The influence of the grain size on the G-ratio does not seem to be significant. For the grain shape M, higher G-ratios are achieved by using the grain d_g= 25 µm. In contrast, for grain L, the use of the smaller grain size d_g = 15 µm leads to higher G ratios. This is attributed to the friability of the respective diamond grain shape. With grain diameter d_g = 15 µm, the average grain density in the contact zone is about 150% higher than with grit diameter d_g = 25 µm. Thus, the single grain load decreases with a reduced grain diameter. In the case of

the very friable grain shape L, this leads to slower wear of the grain. Consideration of the surface parameters and process variables has shown that grain L, d_g = 25 µm has a high wear rate and flattens early in the grinding process. Flattened diamond grains are released from the vitrified bond and lead to profile wear. Profile wear directly results in a low G-ratio. Furthermore, for a small grain size, the release of a worn diamond grain results in lower profile wear than for a large grit size. The volume of a single grain is lower than at higher grain size. Therefore, for grain size d_g= 15 µm, higher G-ratios are measured than for grain size d_g = 25 µm for grain shape L.

Grain shape M is mechanically more stable than grain shape L. As the observation of the surface parameters has shown, this diamond grain shape flattens less than grain shape L. Thus, the grain breakout is lower for grain shape M than for grain shape L. The mechanically stable grain M, d_g = 25 µm splinters in grinding contact instead of flattening. Thus, new sharp cutting edges are generated, which are involved in the material removal. The individual diamond grain is able to remove a larger volume of material. Since less grain breakout is to be expected, the profile wear is also lower for grit shape M than for grain shape L.

An increase of the grain concentration C leads to a decrease of the G ratio for both grain types. At the same porosity, an increase in grain concentration C leads to a reduced bond proportion in the abrasive layer. However, grinding of PcBN is characterized by high mechanical grain loads. Consequently, the lower bond proportion cannot resist the mechanical load and breaks earlier in the process. As a result, abrasive grains are released from the abrasive layer prematurely.

4. Conclusions and Outlook

In this study, the wear mechanism of vitrified bonded diamond grinding wheels is presented for the grinding of PcBN with medium cBN content. The main wear mechanism is grain dulling. In contrast, clogging of the chip space is hardly observed in the high porosity grinding tools. After a material removal of V'_w > 13 mm^3/mm, the abrasive layer topography, the cutting energy and the grinding forces reach a constant level due to an equilibrium of the microwear mechanisms. This equilibrium of microwear and grain breakout leads to a constant grinding ratio G. The friability of the diamond abrasive grain has a significant influence on the course of wear with increasing material removal rate. A high degree of sheared off grains in contact with the very hard PcBN leads to strong flattening of the grain and thus to increased wear of the grinding tool. A less friable grain generates new cutting edges through grain splintering, which enable efficient material removal. Furthermore, as the grain size increases, the grinding forces decrease and the grinding force ratio μ increases. With increasing grain size, the undeformed chip thickness increases, so that the share of friction in the grinding energy e_c decreases. This leads to lower absolute tangential forces F'_t. In relation to the normal force F'_n, however, these tangential forces are higher, since the force component resulting from the cutting of the PcBN material is higher. Additionally, high (31.25%) and very high (37.5%) grain concentrations have been investigated. It is shown that at C = 37.5%vol the bond is overstrained. This leads to increased grain breakout and thus increased profile and edge wear.

Profile wear on the grinding tool can be significantly reduced by selecting semi-friable diamond grain. The G-ratio can be more than tripled compared to previous results for plunge face grinding. As a result of the low profile wear the productive grinding of complex PcBN surfaces is possible. Therefore, a substitution of the spark erosion removal process by a grinding process appears possible for the flute machining of solid PcBN shank tools. Thus, future investigations will focus on the achievable surface quality and the variation of the process parameters.

Conflict of Interest

The authors declare no conflict of interest.

Author Contributions

Berend Denkena: Funding acquisition, Project administration, Supervision, Writing - review & editing, Resources. Alexander Krödel-Worbes: Project administration, Writing - review & editing, Validation, Conceptualization. Dominik Müller-Cramm: Visualization, Writing - review & editing, Writing - original draft, Data curation, Investigation, Formal analysis, Methodology. All authors have approved the final version.

Acknowledgment

The results were obtained within the framework of Project 20863 N of the "Förderung der instustriellen Gemeinschaftsforschung (IGF)", supervised by the "FGW Forschungsgemeinschaft Werkzeuge und Werkstoffe e. V.". The project is funded by the German Federal Ministry for Economic Affairs and Energy (Bundesministerium für Wirtschaft und Energie) on the basis of a resolution of the German Bundestag.

References

[1] Carolan, D., Ivanković, A., & Murphy, N. (2012). Thermal shock resistance of polycrystalline cubic boron nitride. *Journal of the European Ceramic Society, 32(10),* 2581–2586.

[2] Monteiro, S. N., Skury, A. L. D., de Azevedo, M. G., & Bobrovnitchii, G. S. (2013). Cubic boron nitride competing with diamond as a superhard engineering material – an overview. *Journal of Materials Research and Technology, 2(1*), 68–74.

[3] Arsecularatne, J. A., Zhang, L. C., & Montross, C. (2006) Wear and tool life of tungsten carbide, PCBN and PCD cutting tools. *International Journal of Machine Tools and Manufacture, 46(5),* 482–491.

[4] Kress, J. (2007). Auswahl und Einsatz von polykristallinem kubischem Bornitrid beim Drehen, Fräsen und Reiben. *Dr.-Ing. Dissertation*, Technische Universität Dortmund, Germany.

[5] Bömcke, A. (1989). Ein Beitrag zur Ermittlung der Verschleißmechanismen beim Zerspanen mit hochharten polykristallinen Schneidstoffen. *Dr.-Ing. Dissertation*, RWTH Aachen, Germany.

[6] Hooper, R. M., Guillou, M.-O., & Henshall, J. L. (1991). Indentation Studies of cBN-TiC Composites. *Journal of Hard Materials,* 2(3-4), 223–231.

[7] Uesaka, S., & Sumiya, H. (1999). Mechanical properties and cutting performances of high purity polycristalline CBN compact. *Manufacturing Science and Engineering*, *10*, 759–766.

[8] Großmann, G. (1997). Bevorzugte Anwendungsgebiete für PKB-Schneidstoffe. *VDI Berichte – Spezial Werkzeuge*, 18–22.

[9] Friemuth, T. (2002). Herstellung spanender Werkzeuge, Habilitation, Leibniz Universität Hannover, *VDI-Fortschritt-Berichte*, *615*, VDI-Verlag Düsseldorf, Germany.

[10] Malkin, S., & Guo, C. (2008). Grinding technology: Theory and applications of machining with abrasives, 2nd ed, NY: Industrial Press, New York.

[11] Denkena, B., Grove, T., Behrens, L., & Müller-Cramm, D. (2020). Wear mechanism model for grinding of PcBN cutting inserts. *Journal of Materials Processing Technology*, 277, 116474.

[12] Denkena, B., Grove, T., & Behrens, L. (2015). Significant influence factors on the grinding tool wear and cutting mechanisms during grinding of PCBN inserts. *Production Engineering*, 9(2), 187–93.

[13] Azarhoushang, B., Stehle, T., Frank, H. K., & Möhring, H. C. (2017). Effects of grinding process parameters on the surface topography of PCBN cutting inserts. *International Journal of Abrasive Technology*, 8(2), 121–132.

[14] Denkena, B., Grove, T., Müller-Cramm, D., & Krödel, A. (2020). Influence of the cutting direction angle on the tool wear behavior in face plunge grinding of PcBN. *Wear*, 454–455, 203325.

[15] Schindler, F. (2015). Zerspanungsmechanismen beim Schleifen von polykristallinem Diamant. *Dr.-Ing. Dissertation*, RWTH Aachen, Germany.

[16]Vits, F., Trauth, D., Mattfeld, P.-M., & Klocke, F. (2018). Schleifscheibenverschleiß bei der PKD-Bearbeitung: Schleifscheibenverschleißmechanismen beim Schleifen von polykristallinem Diamant, *wt Werkstattstechnik Online*, *108(6)*, 448–453.

[17] Bergs, T., Müller, U., Vits, F., & Barth, S. (2020). Grinding wheel wear and material removal mechanisms during grinding of polycrystalline diamond. *Procedia CIRP*, 93, 1520–1525.

[18] Mitsubishi Materials. (2009). CBN end mill series, the ultimate choice for finish machining moulds. *Tools News 2-2009*.

Berend Denkena is the head of the Institute of Production Engineering and Machine Tools at the Leibniz Universität Hannover

After obtaining doctorate from the Faculty of Mechanical Engineering at the Leibniz Universität Hannover in 1992, he worked as a design engineer and head of various research groups for Thyssen Production Systems both in Germany and the United States. From 1996 to 2001 he was the head of Engineering and Turning Machine Development at Gildemeister Drehmaschinen in Bielefeld. Since 2001 he has been a full professor of Production Engineering and Machine Tools and director of the Institute of Production Engineering and Machine Tools at the Leibniz Universität Hannover.

Prof. Denkena is a CIRP Fellow member. His primary areas of research are geometry and functionalizing manufacturing processes, machine tools for cutting and grinding, production planning and control, and simulation of manufacturing processes.

Alexander Krödel-Worbes is the head of the Department “manufacturing processes” of the Institute of Production Engineering and Machine Tools at the Leibniz Universität Hannover, where he is responsible for over 30 researcher engineers. In 2014, he joined the IFW in the department of manufacturing processes. He was responsible for the group “cutting technologies” from 2016 on.

Dominik Müller-Cramm M.Eng. is research assistant of the Institute of Production Engineering and Machine Tools at the Leibniz Universität Hannover since 2017. His research activities are focused on tool grinding processes of brittle-hard cutting materials.